Research Square

Preprints are preliminary reports that have not undergone peer review.
They should not be considered conclusive, used to inform clinical practice,
or referenced by the media as validated information.

Modulation of Oxidative Stress and Apoptosis by Alteration of Bioactive Lipids in The Pancreas, and Effect of Zinc Chelation in a Rat Model of Alzheimer's Disease

Alev Duygu Acun

duyguacun@akdeniz.edu.tr

Akdeniz University

Deniz Kantar

Akdeniz University

Research Article

Keywords: Alzheimer's Disease, Cyclo-Z, Ceramide, Amylin, Apoptosis, Oxidative Stress

Posted Date: March 4th, 2024

DOI: https://doi.org/10.21203/rs.3.rs-3993800/v1

License: This work is licensed under a Creative Commons Attribution 4.0 International License.
Read Full License

Additional Declarations: No competing interests reported.

Version of Record: A version of this preprint was published at Journal of Trace Elements in Medicine and Biology on June 1st, 2024. See the published version at https://doi.org/10.1016/j.jtemb.2024.127480.

Abstract

Increasing epidemiological evidence highlights the association between systemic insulin resistance and Alzheimer's disease (AD). It is known that peripheral insulin resistance in the early stages of AD precedes and is a precursor to amyloid-β (Aβ) deposition. Although it is known that improving the CNS insulin sensitivity of AD patients is an important therapeutic goal and that the majority of insulin in the brain comes from the periphery, there has been little attention to the changes that occur in the pancreatic tissue of AD patients. Therefore, it is crucial to elucidate the mechanisms affecting insulin resistance in pancreatic tissue in AD. It is known that zinc (Zn+2) chelation is effective in reducing peripheral insulin resistance, cell apoptosis, cell death, and oxidative stress. Aims: This study aimed to determine the bioactive lipids in the pancreas in the Aβ oligomer-induced rat model to determine the changes in amylin (AIPP), oxidative stress, and apoptosis in pancreatic cells and to reveal the therapeutic effect of the Cyclo-Z agent on them. AD and ADC rats were intracerebroventricular (i.c.v.) Aβ1-42 oligomers. Cyclo-Z gavage was applied to ADC and SHC rats for 21 days. First of all, the effects of AIPP, bioactive ceramides, apoptosis and oxidative stress on the pancreatic tissue of AD group rats were evaluated. Then, the effect of Cyclo-Z treatment on these was examined. ELISA kit was used in biochemical analyses. AIPP and ceramide (CER) levels and CER/ sphingosine-1 phosphate (S1P) ratio were increased in the pancreatic tissue of AD rats. It also increased the level of CER kinase (CERK), which is known to increase the concentration of CER 1-phosphate (C1P), which is known to be toxic to cells in the presence of excessive CER concentration. Due to the increase in CER level, it was observed that apoptosis and oxidative stress increased in the pancreatic cells of AD group rats. Cyclo-Z, which has Zn+2 chelating properties, reduced AD model rats' AIPP level and oxidative stress and could prevent pancreatic apoptosis. Similar therapeutic effects were not observed in the pancreatic tissue of Cyclo-Z administered to the SH group. For this reason, it is thought that Cyclo-Z agent may have a therapeutic effect on the peripheral hyperinsulinemia observed in the early stages of AD disease and the resulting low amount of insulin transported to the brain, by protecting pancreatic cells from apoptosis and oxidative stress by regulating their bioactive metabolites.

1. Introduction

Type-2 diabetes (T2D) increases the risk of Alzheimer's disease (AD) type dementia and the conversion from mild cognitive impairment to dementia. However, the mechanisms linking T2D to AD are largely unknown. It is well established that impaired glucose metabolism, insulin resistance, inflammation, oxidative stress; amyloid, amylin (IAPP) and advanced glycosylation end-product accumulation, and mitochondrial dysfunction are biological events that occur in both T2D and AD [1]. This is why AD has recently been called "type-3 diabetes" [2] or "diabetes of the brain" [3]. However, the existence of common molecular mechanisms underlying these events and the involvement of possible common triggers remain largely unknown. It has recently been thought that lipotoxicity may contribute to neurological dysfunction and neurodegeneration, possibly representing the missing link in the pathogenetic mechanisms linking T2D to AD. Lipotoxicity can lead to insulin resistance, oxidative stress, ceramide (CER), and amyloid accumulation, which are common biological events in the pathogenesis of T2D and

AD. Interestingly, the pathways of lipotoxicity-induced damage are very similar in all tissues involved in the pathogenesis of both T2D and AD [1]. Therefore, elucidating the common molecular pathways activated by lipotoxicity in T2D and AD may lead to new therapeutic perspectives.

CERs are considered potential lipotoxic molecules with the ability to modulate cellular metabolism [4]. Pancreatic β-cell lipotoxicity caused by CER accumulation was first demonstrated in 1998 [5]. CER catabolism is controlled by ceramidases, which reduce CER to free fatty acids and sphingosine that can be further phosphorylated by sphingosine kinase and produce sphingosine-1 phosphate (S1P). CER and S1P are bioactive lipids downstream of the sphingolipid pathway and play important roles in cell signaling. In physical conditions, they play opposite roles in cellular metabolism. Although CER is known to be involved in stress-related cellular responses and apoptosis; S1P stimulates cell survival, proliferation, and tissue regeneration. Therefore, cells need to maintain the balance between CER and S1P [6]. At the same time; phosphorylation of CER by CER kinase (CERK) produces CER 1-phosphate (C1P), which has the opposite effects of CER and is a key regulator of cell homeostasis. To date, the only enzyme identified to induce C1P biosynthesis is CERK [7]. However, it has been noticed that there are changes in CER levels in pathological conditions such as AD and T2D [6]. Changes in SL metabolism enzymes observed at different stages of AD lead to an increase in CER levels (pro-apoptotic) and a decrease in S1P and C1P (anti-apoptotic). In this case, it may determine or promote cell fate in the pathophysiology of AD [7]. CER deposition-induced lipotoxicity is a mechanism also involved in the pathogenesis of AD. In the early stages of Alzheimer's disease, increased CER levels have been observed in the brains of AD patients [8], and high serum CER levels may increase the risk of developing AD [9]. Moreover, insulin resistance, mainly caused by lipotoxicity, is known to be actively involved in the pathophysiology of AD. Peripherally synthesized CERs can cross the blood-brain barrier (BBB), alter insulin signaling, and induce insulin resistance in the brain. [1]. It has been shown that the increase in CERs in rat pancreatic islets leads to impaired insulin secretion as well as a decrease in the proliferative capacity of β-cells [10]. Pancreatic beta cells are characterized by low expression of antioxidant enzymes, so they are more vulnerable to oxidative stress. At the same time, many studies show that lipotoxicity induces β-cell oxidative stress, thereby impairing β-cell function and survival [1]. Therefore, reducing CER levels in the pancreas can be considered an important therapeutic target in the pathogenesis of AD disease.

At the same time, the increase in insulin secretion demand due to insulin resistance leads to the overproduction of pancreatic islet amyloid polypeptide (IAPP), also known as amylin, which accumulates and tends to form aggregates [11]. IAPP, a pancreatic β-cell hormone co-secreted with insulin, is expressed mainly in the pancreas. Although not expressed in the brain, people with AD have increased concentrations of IAPP in the blood, cerebrospinal fluid (CSF), and brain parenchyma. It has been found that intravenously injected IAPP enters the mouse brain and is taken up by neurons and microglia, contributing to AD pathology [12]. İnsulin resistance and the resulting increase in demand for insulin secretion leads to overproduction of IAPP and tends to accumulate and form aggregates [1]. Remarkably, IAPP aggregates can induce oxidative stress and apoptosis, thus being cytotoxic to beta-cells [11, 13, 14]. Increased apoptotic rate of β-cells is also associated with increased CER levels in

pancreatic islets [15]. Therefore, we can conclude that AIPP accumulation, which develops due to CER accumulation in the pancreas, causes pancreatic β-cells and further exacerbates insulin resistance.

It has been shown that Zn^{+2} chelation can reverse Zn^{+2}-induced expression level and accumulation and is also effective in reducing cell apoptosis cell death and oxidative stress [16]. Additionally, it has been shown that the mitogenic effects of S1P can be enhanced by a Zn^{+2}-dependent mechanism [17]. Cyclo (His-Pro) (CHP) has a chelating effect on Zn^{+2} and assists Zn^{+2} transport via an intestinal CHP transport mechanism independent of the normal elemental Zn^{+2} transport system [18]. CHP is a metabolite of thyrotropin-releasing hormone (TSH) containing the amide chemical formula PGlu-His-Pro [19]. CHP is ubiquitous in the CNS, blood, and gastrointestinal tract as well as several body fluids [20], and is a cyclic form of two amino acids, L-histidine and proline [21]. This cyclic form is also required for active transport through the gut [22] and the BBB [23–25]. While the therapeutic application of Zn^{+2} or CHP alone in the control of blood glucose levels is minimally effective; Cyclo-Z, the form in which CHP and Zn^{+2} are applied together, has been very effective [18]. Cyclo-Z treatment given to amyloid-beta (Aβ) oligomer (AβO)-induced Alzheimer rats has been shown to have a positive effect on peripheral insulin resistance and brain insulin pathway [26]. The effect of Cyclo-Z treatment on pancreatic lipotoxicity, defined as the common molecular mechanism of T2D and AD disease, is unknown. Therefore, it is crucial to elucidate the effect of Cyclo-Z treatment on bioactive lipids in the pancreas and the resulting insulin resistance and oxidative stress mechanisms.

2. Material and Methods

2.1. Animal preparation

3 months male albino Wistar rats weighing 250–300 g were obtained from Akdeniz University Animal Care Unit. Groups of 4 rats per cage were housed in stainless steel cages and given food and water ad libitum. Animals were kept at a constant temperature of 23 ± 1°C and subjected to a 12-hour light-dark cycle. The animals were divided into four groups with 8 animals in each group. 1) sham surgery (1.25 µl DMSO + 8.75 µl PBS/10µl) intracerebroventricular (i.c.v) injection plus water gavage (SH); (2) sham surgery (1,25 µl DMSO + 8,75 µl PBS/10µl) i.c.v. injection plus Cyclo-Z gavage (10 mg Zn/kg and 0,2 mg SHP/kg) (SHC); (3) Aβ42 oligomer (2,5 nmol/10 µl) i.c.v. injection plus water gavage (AD); (4) Aβ42 oligomer (2,5 nmol/10 µl) i.c.v. injection plus Cyclo-Z gavage (10 mg Zn/kg and 0,2 mg SHP/kg) (ADC).

Aβ1–42 oligomers have been prepared according to the literature [27]. Aβ1–42 (Sigma-Aldrich, USA, product no: A9810) peptides were dissolved in DMSO to a concentration of 2 mmol. It was then diluted 8 times in sterile PBS and vortexed for 30 minutes at room temperature. It is then centrifuged at 15000xg for 1 hour at 4°C. Supernatants (250 µl) were aliquoted (25 µl) and frozen at -20°C. Aβ1–42 oligomers were used within 24 hours after leaving them at 4°C. Sham groups were given i.c.v. 10 µl of solution prepared with 1.25 µl of DMSO and 8.75 µl of PBS. Cyclo was purchased from Santa Cruz with the molecular formula C11H14N4O2 and a molecular weight of 234.26 g/mol (Santa Cruz Biotechnology,

Europe). Zinc chloride with purity > 98% was purchased from Molar Kimya (MZK.100310.1000). Previous publications are referenced for Cyclo-Z dosage [28]. To obtain this dose, 50 mg of Cyclo and 2.5 g of Zn were dissolved in 1 L of water.

Rats were anesthetized with a combination of ketamine (80 mg/kg, i.p.) and xylazine (5 mg/kg, i.p.). Then, a rat model of AD was created by placing it in a standard stereotaxic device [29, 30]. A mid-sagittal incision was made in the scalp and the skull was drilled bilaterally using a dental drill on the lateral ventricles (AP: -0.8 mm, ML:±1.4 mm, DV: -4.0 mm). Aβ-42 oligomers were injected into rats in AD and ADC groups, and a solution was prepared with DMSO + PBS in SH and SHC groups at a rate of 0.5 µl/min. The Hamilton syringe was removed 5 minutes after the injection. After the operation, the scalp was sutured closed. In addition, sulfamethoxazole was sprinkled over the suture to prevent infection, and penicillin (40,000 U) was injected intramuscularly once a day for 3 days. Gavage was applied for 21 days after i.c.v. injections.

2.2. Biochemical İnvestigations

Pancreatic tissues were obtained for sandwich ELISA (n = 6–8) per group analyses. For biochemical measurements, pancreatic tissues were taken under anesthesia and animals were sacrificed. The excised pancreatic tissues were frozen in liquid nitrogen and stored at -80°C. Tissue samples were weighed and then homogenized on ice in PBS based on homogeneous tissue weight (PRO 200 Homogenizer, PRO Scientific Inc., Connecticut, USA). Homogenized samples were centrifuged at 2000–3000 RPM at 4°C for 20 minutes. The resulting supernatants were separated and stored at -80°C.

2.2.1. Measurement of AIPP Levels in Pancreatic Tissue Homogenates

According to the manufacturer's instructions, AIPP levels in the supernatants of pancreas homogenates were measured using a commercially available sandwich ELISA kit (SunRed-SRB-T-87752). AIPP was added to wells pre-coated with AIPP monoclonal antibody and then incubated. Biotin-labeled anti-AIPPantibodies were added to combine with streptavidin-HRP. After incubation and washing, unbound components are removed and substrate solutions A and B are added. The substrate solution reacts with the HRP enzyme, leading to color formation in the wells containing Amylin. The substrate solution reacts with the HRP enzyme, resulting in color formation in the wells proportional to the amount of Amylin. The reaction is terminated by adding an acidic stop solution. OD is measured spectrophotometrically at 450 nm. The sample amount of AIPP is calculated with a standard curve plot.

2.2.2. Measurement of CER Levels in Pancreatic Tissue Homogenates

According to the manufacturer's instructions, CER levels in the supernatants of pancreas homogenates were measured using a commercially available sandwich ELISA kit (SunRed-201-11-4776). CER was added to wells pre-coated with CER monoclonal antibody and then incubated. Biotin-labeled anti-CER

antibodies were added to combine with streptavidin-HRP. After incubation and washing, unbound components are removed and substrate solutions A and B are added. The substrate solution reacts with the HRP enzyme, leading to color formation in the wells containing CER. The substrate solution reacts with the HRP enzyme, resulting in color formation in the wells proportional to the amount of CER. The reaction is terminated by adding an acidic stop solution. OD is measured spectrophotometrically at 450 nm. The sample amount of CER is calculated with a standard curve plot.

2.2.3. Measurement of CERK Levels in Pancreatic Tissue Homogenates

CERK levels in the supernatants of pancreas homogenates were measured using a commercially available sandwich ELISA kit (SunRed-201-11-2001) by the manufacturer’s instructions. CERK was added to wells pre-coated with CERK monoclonal antibody and then incubated. Biotin-labeled anti-CERK antibodies were added to combine with streptavidin-HRP. After incubation and washing, unbound components are removed and substrate solutions A and B are added. The substrate solution reacts with the HRP enzyme, leading to the color formation in the wells containing CERK. The substrate solution reacts with the HRP enzyme, resulting in color formation in the wells proportional

to the amount of CERK. The reaction is terminated by adding an acidic stop solution. OD is measured spectrophotometrically at 450 nm. The sample amount of CERK is calculated with a standard curve plot.

2.2.4. Measurement of S1P Levels in Pancreatic Tissue Homogenates

According to the manufacturer's instructions, S1P levels in the supernatants of pancreas homogenates were measured using a commercially available sandwich ELISA kit (SunRed-201-11-1805). S1P was added to wells pre-coated with S1P monoclonal antibody and then incubated. Biotin-labeled anti-S1P antibodies were added to combine with streptavidin-HRP. After incubation and washing, unbound components are removed and substrate solutions A and B are added. The substrate solution reacts with the HRP enzyme, leading to color formation in the wells containing S1P. The substrate solution reacts with the HRP enzyme, resulting in color formation in the wells proportional to the amount of S1P. The reaction is terminated by adding an acidic stop solution. OD is measured spectrophotometrically at 450 nm. The sample amount of S1P is calculated with a standard curve plot.

2.2.5. Measurement of Total Oxidant Status (TOS) Levels in Pancreatic Tissue Homogenates

The manufacturer's instructions measured TOS levels in the supernatants of pancreas homogenates using a commercially available sandwich ELISA kit (SunRed-201-11-1669). TOS was added to wells pre-coated with TOS monoclonal antibody and then incubated. Biotin-labeled anti-TOS antibodies were added to combine with streptavidin-HRP. After incubation and washing, unbound components are removed and substrate solutions A and B are added. The substrate solution reacts with the HRP enzyme,

leading to color formation in the wells containing TOS. The substrate solution reacts with the HRP enzyme resulting in color formation in the wells proportional to the amount of TOS. The reaction is terminated by adding an acidic stop solution. OD is measured spectrophotometrically at 450 nm. The sample amount of TOS is calculated with a standard curve plot.

2.2.6. Measurement of 4-Hydroxynonenal (4HNE) Levels in Pancreatic Tissue Homogenates

According to the manufacturer's instructions, 4HNE levels in the supernatants of pancreas homogenates were measured using a commercially available sandwich ELISA kit (SunRed-201-11-0813). 4HNE was added to wells pre-coated with 4HNE monoclonal antibody and then incubated. Biotin-labeled anti-4HNE antibodies were added to combine with streptavidin-HRP. After incubation and washing, unbound components are removed and substrate solutions A and B are added. The substrate solution reacts with the HRP enzyme, leading to color formation in the wells containing 4HNE. The substrate solution reacts with the HRP enzyme, resulting in color formation in the wells proportional to the amount of 4HNE. The reaction is terminated by adding an acidic stop solution. OD is measured spectrophotometrically at 450 nm. The sample amount of 4HNE is calculated with a standard curve plot.

2.2.7. Measurement of Caspase-3 Levels in Pancreatic Tissue Homogenates

Caspase-3 levels in the supernatants of pancreas homogenates were measured using a commercially available sandwich ELISA kit (SunRed-201-11-0281) according to the manufacturer’s instructions. Caspase-3 was added to wells pre-coated with Caspase-3 monoclonal antibody and then incubated. Biotin-labeled anti-Caspase-3 antibodies were added to combine with streptavidin-HRP. After incubation and washing, unbound components are removed and substrate solutions A and B are added. The substrate solution reacts with the HRP enzyme, leading to color formation in the wells containing Caspase-3. The substrate solution reacts with the HRP enzyme resulting in color formation in the wells proportional to the amount of Caspase-3. The reaction is terminated by adding an acidic stop solution. OD is measured spectrophotometrically at 450 nm. The sample amount of Caspase-3 is calculated with a standard curve plot.

2.2.8. Measurement of Glutathione (GSH) Levels in Pancreatic Tissue Homogenates

The manufacturer's instructions measured GSH levels in the supernatants of pancreas homogenates using a commercially available sandwich ELISA kit (SunRed-201-11-7122). GSH was added to wells pre-coated with GSH monoclonal antibody and then incubated. Biotin-labeled anti-GSH antibodies were added to combine with streptavidin-HRP. After incubation and washing, unbound components are removed and substrate solutions A and B are added. The substrate solution reacts with the HRP enzyme, leading to color formation in the wells containing GSH. The substrate solution reacts with the HRP enzyme resulting in color formation in the wells proportional to the amount of GSH. The reaction is

terminated by adding an acidic stop solution. OD is measured spectrophotometrically at 450 nm. The sample amount of GSH is calculated with a standard curve plot.

2.3. Statistical analysis

Statistical ananalyses of the data obtained at the end of the study were performed with the SPSS 23.0 for Windows (SPSS, Chicago, IL, USA) program. Statistical comparisons of data obtained from biochemical analyses between groups were made using one-way ANOVA and post hoc Tukey test. Results are expressed as mean ± standard error. Significance levels were set at $P < 0.05$. All experimenters were blinded to animal experimental group membership during data collection and analysis.

3. Results

3.1. Pancreas AIPP Levels

The mean values of pancreatic AIPP levels are given in Fig. 1A. There was a statistically significant difference in pancreatic AIPP levels between groups [$F(3,20) = 5.798$, $p < 0.01$]. The pancreatic levels were significantly increased in the AD (47.35 ± 5.66 ng/g protein) versus the SH (26.44 ± 2.21 ng/g protein)($p < 0.01$) and SHZ (31.94 ± 2.77 ng/g protein)($p < 0.05$). However, a slight decrease was seen in the pancreatic levels of the ADC (36.32 ± 3,09 ng/g protein) group compared to the AD group. This decrement did not reach a significant level. However, the pancreatic level of the ADC group was not significantly different from the SH group.

3.2. Pancreas CER Levels

The mean values of pancreatic CER levels are given in Fig. 1B. There was a statistically significant difference in pancreatic CER levels between groups [$F(3,20) = 17.704$, $p < 0.001$]. The pancreatic CER levels were significantly increased in the AD (6242.78 ± 413,85 ng/g protein) versus the SH (2548,9 ± 237,69 ng/g protein)($p < 0.001$). The pancreatic CER levels were significantly increased in the ADC (4412,8 ± 382,29 ng/g protein) versus the SH ($p < 0.05$). Although the CER level of the ADC group was significantly higher than that of the SH ($p < 0.05$) and SHC (3018,5±,497,93 ng/g protein) ($p < 0.01$) groups, it was significantly lower compared to the AD group ($p < 0.05$).

3.3. Pancreas CERK Levels

The mean values of pancreatic CERK levels are given in Fig. 1C. There was a statistically significant difference in pancreatic CERK levels between groups [$F(3,20) = 14.157$, $p < 0.001$]. The pancreatic CERK levels were significantly increased in the AD (10.90 ± 1.14 ng/mg protein) versus the SH (4.46 ± 0.38 ng/mg protein)($p < 0.001$). No significant difference was found between the ADC (6.69 ± 0.69 ng/mg protein) group and the SH group. The pancreatic CERK levels were significantly decreased in the ADC versus the AD ($p < 0.01$). However, a slight increase was seen in the pancreatic CERK levels of the SHC

(5.89 ± 0.46 ng/mg protein) group compared to the SH group. This increment did not reach a significant level.

3.4. Pancreas S1P Levels

The mean values of pancreatic S1P levels are given in Fig. 1D. There was a statistically significant difference in pancreatic S1P levels between groups [$F(3,20) = 4.429$, $p < 0.05$]. The pancreatic S1P levels were significantly increased in the AD (45.82 ± 4.82 ng/g protein) versus the SH (28.79 ± 2.52 ng/g protein) ($p < 0.05$). The pancreatic S1P levels were significantly increased in the ADC (47.03 ± 0.38 ng/g protein) versus the SH ($p < 0.05$). However, a slight increase was seen in the pancreatic S1P levels of the SHC (38.67 ± 3.25 ng/g protein) group compared to the SH group. This increment did not reach a significant level. No significant difference was found between the ADC group and the AD group.

3.5. Pancreas CER/S1P Ratio

The mean values of pancreatic CER/S1P ratio are given in Fig. 1E. There was a statistically significant difference in pancreatic CER/S1P ratio between groups [$F(3,20) = 3.271$, $p < 0.05$]. The CER/S1P ratio of the AD group (146.99 ± 20.70) rats tends to increase, although it is not significant, compared to the SH group (92.61 ± 13.03); but it is significantly higher than that of the SHP group (82.17 ± 16.01, $p < 0.05$). At the same time, it was found that the CER/S1P ratio of the ADC group(98.03 ± 12.58) tended to decrease compared to the AD group, although it was not significant. Additionally, the CER/S1P ratio of the ADC group was not found to be different from the SH group.

3.6. Pancreas Total Oxidant Status (TOS) Levels

The mean values of pancreatic TOS levels are given in Fig. 2A. There was a statistically significant difference in pancreatic TOS levels between groups [$F(3,20) = 3.939$, $p < 0.05$]. The pancreatic TOS levels were slightly increased in the AD (0.53 ± 0.07 nmol/mg protein) versus the SH (0.38 ± 0.03 nmol/mg protein). This increment did not reach a significant level. The pancreatic TOS levels were significantly decreased in the ADC (0.30 ± 0.03 nmol/mg protein) versus the AD ($p < 0.05$). No significant difference was found between the SHC (0.34 ± 0.04 nmol/mg protein) group and the SH group.

3.7. Pancreas 4-Hydroxynonenal (4HNE) Levels

The mean values of pancreatic 4HNE levels are given in Fig. 2B. There was a statistically significant difference in pancreatic 4HNE levels between groups [$F(3,20) = 7.195$, $p < 0.01$]. The pancreatic 4HNE levels were significantly increased in the AD (2.54 ± 0.33 pg/mg protein) versus the SH (1.15 ± 0.14 pg/mg protein) ($p < 0.01$) and SHC (1.57 ± 0.13 pg/mg protein) ($p < 0.05$). The pancreatic 4HNE levels were significantly increased in the ADC (2.09 ± 0.21 pg/mg protein) versus the SH ($p < 0.05$). The pancreatic 4HNE levels were slightly decreased in the ADC versus the AD. This decrement did not reach a significant level. No significant difference was found between the SHC group and the SH group.

3.8. Pancreas Caspase-3 Levels

The mean values of pancreatic Caspase-3 levels are given in Fig. 2C. There was a statistically significant difference in pancreatic Caspase-3 levels between groups [$F(3,20) = 14.661$, $p < 0.001$]. The pancreatic Caspase-3 levels were significantly increased in the AD (0.35 ± 0.04 ng/mg protein) versus the SH (0.16 ± 0.02 ng/mg protein) and SHC (0.11 ± 0.02 ng/mg protein). The pancreatic Caspase-3 levels were significantly decreased in the ADC (0.14 ± 0.008 ng/mg protein) versus the AD ($p < 0.001$ for all comparisons). No significant difference was found between the SHC group and the SH group. No significant difference was found between the ADC group and the SH group.

3.9. Pancreas Glutathione (GSH) Levels

The mean values of pancreatic GSH levels are given in Fig. 2D. There was a statistically significant difference in pancreatic GSH levels between groups [$F(3,20) = 6.449$, $p < 0.01$]. The pancreatic GSH levels were significantly increased in the AD (0.22 ± 0.01 mg/g protein) versus the SH (0.16 ± 0.01 mg/g protein). The pancreatic GSH levels were significantly increased in the SHC (0.21 ± 0.008 mg/g protein) versus the SH ($p < 0.05$ for all comparisons). The pancreatic GSH levels were significantly increased in the AHC (0.23 ± 0.01 mg/g protein) versus the SH ($p < 0.01$). No significant difference was found between the AHC group and the AH group.

3.10. Correlations between pancreas CER levels and pancreas AIPP levels

Significant correlations were found between changes in the pancreas AIPP levels and pancreas CER levels (Fig. 3A). There was a positive correlation between the pancreas AIPP and CER levels (Pearson $r = 0.663$, $p < 0.001$, $N = 24$).

3.11. Correlations between pancreas CER levels and pancreas CERK levels

Significant correlations were found between changes in the pancreas CER levels and pancreas CERK levels (Fig. 3B). There was a positive correlation between the pancreas CER and CERK levels (Pearson $r = 0.754$, $p < 0.001$, $N = 24$).

3.12. Correlations between pancreas S1P levels and pancreas GSH levels

Significant correlations were found between changes in the pancreas S1P levels and pancreas GSH levels (Fig. 3C). There was a positive correlation between the pancreas S1P and GSH levels (Pearson $r = 0.624$, $p < 0.001$, $N = 24$).

4. Discussion

It is important to investigate the pathological changes seen in the early stages of AD disease [31]. Aβ can bind to the insulin receptor competitively and induce insulin resistance [32]. Studies have also found

that hyperglycemia and hyperinsulinemia, which develop in the initial stages of AD, maybe early biomarkers of AD [33, 34]. In patients with AD, insulin resistance in the periphery is positively associated with brain Aβ accumulation in the frontal and temporal regions [35]. Therefore, it is vital to learn the mechanisms that trigger peripheral insulin resistance in AD. The central infusion of AβOs leads to peripheral insulin resistance [36]. At the same time, it was found that there was a hyperinsulinemia state against hyperglycemia and peripheral insulin resistance that occurred in the AβO-induced early AD rat model [34]. Considering that chronic peripheral hyperinsulinemia reduces the amount of insulin transported to the brain by suppressing BBB insulin receptors, it is an expected result that patients with AD will reduce brain insulin concentration [37, 34]. Many of the well-documented mechanisms that induce neuronal and synaptic degeneration in the AD brain are triggered and propagated due to the effects of soluble oligomers of the Aβ peptide on neurons and glia [38]. Therefore, our study aimed to examine the changes in the pancreas of the AβO-induced AD rat model. It has also been reported that 20-week-old mice have increased plasma Aβ levels, accompanied by systemic glucose intolerance, insulin resistance, and hyperinsulinemia, before the appearance of amyloid deposits in the brain [39]. It is known that Aβ levels also increase in the pancreas of AD patients [40, 41]. Studies have shown that Aβ is deposited together with IAPP in the pancreas [42, 40, 43]. Pancreatic islet accumulation of Aβ is observed only in the presence of hIAPP [44]. Furthermore, it has been shown that Aβ deposited in the pancreas is not produced from pancreatic APP and probably originates from circulating amyloid peptides [31]. Therefore, increased AIPP in the pancreas of AD group rats may form a fibrillar structure in the pancreas together with plasma Aβ, and high circulating AIPP levels may increase the risk of AD [45]. As a matter of fact, in our study, it was determined that the amount of AIPP in the pancreas of AD group rats increased significantly compared to the SH group. In the progression of AD, accumulation of AIPP has been shown to induce hyperinsulinemia and insulin resistance in AD mice [46, 47]. Therefore, it was concluded that restoring AIPP homeostasis in early AD could reduce AD pathology [48].

At the same time, AD-induced insulin resistance alters lipid homeostasis. Moreover, the role of lipid metabolism in AD progression is well-known [6]. Although the pathogenesis of AD has not yet been fully elucidated, the results of studies show that the bioactive SLs CER and S1P play a role in AD, starting from the earliest prodromal stages. It is well known that CER, the central metabolite of SL metabolism, is a pro-apoptotic molecule. It stimulates inflammation, autophagy, and oxidative stress with mitochondrial dysfunction. Its phosphorylated analog S1P stimulates cell survival, proliferation, and migration. S1P also plays a role in neurodevelopment, synaptic transmission, neuroinflammation, and autophagy [49]. Therefore, even minor changes in CER metabolism in response to various stimuli are decisive for cellular fate [50]. The imbalance of SL species due to dysregulation of SL metabolism is a common event in AD [49]. A study showed that brain CER levels of Alzheimer's patients increased compared to neurologically normal controls of the same age. Increased serum CER levels have also been reported in Alzheimer's patients with mild to moderate symptoms [50]. There is an increase in the serum CER level of AD patients, and in our study, it was observed that the CER level in the pancreatic tissue of AD rats increased significantly compared to the SH group. It also showed that the S1P levels of AD rats increased compared to the SH group. Our findings show that the level of bioactive metabolite S1P increased in the

AD group due to increased CER production. However, the increase in the S1P level is very minor compared to the increase in the CER level. For this, the CER/S1P ratio was examined. It was found that the CER/S1P ratio of the AH group was significantly higher than that of the SH group. To evaluate this situation, the CER/S1P ratio was examined. It was found that the CER/S1P ratio of the AH group was significantly higher than that of the SH group. Since CER is the precursor molecule of S1P synthesis, a change in CER level is expected to affect the level of CER-derived metabolites [51]. It shows that SL metabolism in pancreatic tissue in the early stage of AD is regulated by the combined activation of pro-apoptotic and anti-apoptotic pathways. CER and C1P are antagonistic signals, and C1P can mimic many of the effects of S1P. The only enzyme known to induce the biosynthesis of C1P is CERK. Our study found that the CERK level of AD group rats was significantly increased compared to the SH group. It has been observed that, unlike relatively low concentrations of C1P that stimulate cell growth and inhibit apoptosis, relatively higher concentrations of C1P are toxic and can kill cells. This contradictory observation is explained by the fact that overexpression of CERK in the presence of abnormally high concentrations of CER will cause an excessive increase in intracellular C1P levels, thereby reaching C1P concentrations that are toxic to cells [7]. As a matter of fact, in our study, it was found that the increase in pancreatic CER levels had a significant correlation with the increase in CERK levels. Therefore, the overexpression of CERK at extremely high CER concentrations may explain the situation we encountered in the S1P results.

It is well-established that apoptosis, or programmed cell death, occurs as a result of the accumulation of CER [52]. CER can initiate a series of deleterious changes that lead to apoptotic cell death by various mechanisms, such as increased mitochondria depolarization and permeability, increased ROS production, cytochrome-c release, Bcl-2 depletion, and caspase-3 activation [50]. Studies have shown that neuronal death due to CERs is typically linked to the mitochondrial pathway, which is regulated by caspase-9/caspase-3 [53]. In our study, we found that the level of caspase-3 in the pancreas of rats in the AD group was significantly higher than that in the SH group, indicating a higher incidence of apoptotic cell death in the pancreas of the AD group. The increase in CER levels also stimulates the generation of ROS in a concentration-dependent manner, which can cause oxidative stress and have detrimental consequences for neuronal survival. Oxidative stress occurs when the cellular antioxidant defenses are unable to keep ROS levels below the toxic threshold. In our study, we examined the effect of the significant increase in CER and CER/S1P levels of the AD group compared to the SH group on TOS levels. We observed that TOS levels in the pancreatic tissue of the AD group tended to increase compared to the SH group. Consistent with these findings, we observed a significant increase in the level of 4HNE in the pancreas of the AD group compared to the SH group. The typically toxic end product of ROS-induced lipid peroxidation is 4HNE [50]. Our study observed that the pancreatic 4HNE level of the AD group increased significantly compared to the SH group. Glutathione (GSH) is the most abundant non-protein thiol in mammalian cells and is the most important antioxidant within cells, providing tight control of the cellular redox state. Intracellular GSH depletion is an early sign in the progression of apoptosis. It has been previously reported that depletion of GSH leads to CER production and apoptosis [54]. GSH levels of the AD group were found to be significantly increased compared to the SH group. This

increase in GSH levels indicated a compensatory mechanism, as we observed in the increases in S1P and C1P levels in the early stages of AD disease. It was observed that there was a significant correlation between pancreatic S1P and GSH levels of the AD group.

Previous studies have suggested that relatively high concentrations of Zn^{+2} are required for the normal function of pancreatic β cells. It also showed that Zn^{+2} reduction in pancreatic islets of hIAPP-Tg mice was associated with hyperglycemia [19]. However, it has been shown that Zn^{+2} chelation can reverse the expression level of Zn^{+2}-induced IAPP, and also significantly reduces cell death and caspase-3 activity. Therefore, chelating Zn^{+2} therapy is effective in reducing Zn^{+2}-induced IAPP accumulation and beta-cell apoptosis [16]. Our study determined that the AIPP level of the ADC group tended to decrease compared to the AD group and was not significantly different from the SH group. Additionally, it was shown that there was a significant decrease in the caspase-3 level of the ADC group compared to the AD group and that Cyclo-Z treatment was effective in reducing pancreatic β-cell apoptosis. However, no difference was found in the AIPP and caspase-3 levels of the SHC group compared to the SH group. The CHP therapeutic agent has also been shown to reduce oxidative stress in the pancreas in an STZ-induced rat model [55]. In our study, pancreatic TOS levels of the ADC group decreased significantly compared to the AD group, and 4HNE levels tended to decrease. On the other hand, the increase in GSH levels shown by the AHC group compared to the AH group is compatible with the decrease in oxidative stress. Similarly, Cyclo-Z therapeutic agents administered to healthy rats also tended to reduce pancreatic caspase-3 and TOS levels of the SHP group compared to the SH group. At the same time, the GSH level of the SHP group increased significantly compared to the SH group. In a similar study, Zn^{+2} supplementation was shown to increase GSH levels and reduce lipid peroxidation due to ischemia-reperfusion injury [56]. Based on these results, it was concluded that the Cyclo-Z agent reduces oxidative stress in the pancreas due to GSH, TOS, and 4HNE changes, and may also prevent pancreatic cell apoptosis.

ROS modulates SL metabolism, including enzymes that generate CER and S1P. ROS activates CER-producing enzymes, inducing CER production, leading to apoptosis, and inhibiting S1P production, which promotes survival [57]. Therefore, it seems likely that there will be a change in the levels of CER, S1P, and C1P in pancreatic cells due to the reduction of oxidative stress due to Cyclo-Z treatment in the pancreas. Supporting this, in our study, it was found that the level of CER in the pancreas of the ADC group decreased significantly. At the same time, the pancreatic CERK level was significantly decreased in the ADC group compared to the AD group. Low expression of CERK in the presence of low levels of CER results in relatively low levels of C1P, which stimulates its intracellular growth and is known to inhibit apoptosis [7]. Additionally, cellular production of S1P depends on the activity of the ceramidase enzyme, and there is a Zn^{+2} binding site in the active site of this enzyme. Zn^{+2} is a necessary element for the full function of this enzyme [51]. A study showed that the mitogenic effects of S1P could be increased by a Zn^{+2}-dependent mechanism [17]. In our study, it was observed that the Zn-chelating Cyclo-Z therapeutic agent tended to increase the S1P level of the ADC group in the AD group. At the same time, the ADC group had significantly higher S1P levels than the SH group. Also, Cyclo-Z tended to reduce the CER/S1P ratio of the ADC group compared to the AD group. However, the therapeutic effect of the ADC group of

Cyclo-Z on SL biometabolites in SL metabolism was not observed in the SHC group. Therefore, it has been demonstrated that the therapeutic effect of Cyclo-Z agent is not only on the brain of AD rats but also can protect pancreatic cells from beta-cell apoptosis by regulating SL bioactive metabolites. The emergence of peripheral insulin resistance almost 15 years before Aβ accumulation in AD disease supports the contribution of AD biomarkers to the pathogenesis and reveals insights into the pathogenesis of AD. It is also known that chronic peripheral hyperinsulinemia causes the downregulation of insulin receptors in the BBB and reduces the amount of insulin transported to the brain [58]. Therefore, the therapeutic effect of Cyclo-Z on AD pancreatic β-cells is considered important for the early treatment of the disease.

5. Conclusions

When pathological similarities and common pathogenic mechanisms between T2D and AD are investigated, the connection between both diseases becomes increasingly evident. For this reason, AD is also called “brain diabetes” or “T3D”. This condition has been described as a metabolic syndrome that can lead to progressive brain insulin resistance-related abnormalities resulting in disruption of central insulin signaling processes, neurotoxin accumulation, neuronal stress, and culminating in the process of neurodegeneration. Peripheral insulin resistance seen in the early stages of AD leads to decreased insulin signaling in the CNS and subsequent changes in brain metabolism. Therefore, treatment methods aimed at improving insulin sensitivity may also benefit patients at risk of AD in the early stages. IAPP forms amyloid plaques that play a role in impairing pancreatic islet function and mediating β-cell apoptosis. AIPP was found to accumulate in the pancreas of AD mice, causing hyperinsulinemia and insulin resistance. One of the most important reasons for trying to correct insulin resistance is that it can change lipid homeostasis in the pancreas. Accordingly, it determines the cellular fate by increasing the apoptosis or programmed cell death and oxidative stress of the pancreatic tissue. Therefore, how chronic peripheral hyperinsulinemia seen in the early stages of AD affects the pancreatic tissue and deriving effective therapeutic approaches to prevent it are considered very important for AD disease. Indeed, there are still many questions to be answered about therapeutic strategies derived from this topic.

Declarations

Funding

This study was not supported by any funding.

Conflict of Interest

The authors report no conflicts of interest in this work.

Ethics Approval

Ethical approval for this work was obtained from Akdeniz University Local Committee on Animal Research Ethics (ethics approval date and number: 06.11.2023/2023.11.006).

Availability of Data and Materials

The data supporting this study's findings are available from the corresponding author, upon reasonable request.

Author Contributions

A.D.A. and D.K. generated the rat models. A.D.A. analyzed ELISA's data. A.D. and D.K. wrote the main manuscript text and A.D.A.prepared figures 1-3. A.D.A. and D.K. were involved in data interpretation, critically reviewed and provided their final approval of the manuscript, and agreed to be accountable for the work.

Consent to Participate

Not applicable.

Consent for Publication

Not applicable.

Acknowledgments

Not applicable.

References

1. Marrano N, Biondi G, Borrelli A, Rella M, Zambetta T, Di Gioia L, Caporusso M, Logroscino G, Perrini S, Giorgino F, Natalicchio A (2023) Type 2 Diabetes and Alzheimer's Disease: The Emerging Role of Cellular Lipotoxicity. Biomolecules 13 (1). doi:10.3390/biom13010183
2. de la Monte SM, Wands JR (2008) Alzheimer's disease is type 3 diabetes-evidence reviewed. J Diabetes Sci Technol 2 (6):1101–1113. doi:10.1177/193229680800200619
3. Sebastiao I, Candeias E, Santos MS, de Oliveira CR, Moreira PI, Duarte AI (2014) Insulin as a Bridge between Type 2 Diabetes and Alzheimer Disease - How Anti-Diabetics Could be a Solution for Dementia. Front Endocrinol (Lausanne) 5:110. doi:10.3389/fendo.2014.00110
4. Lipke K, Kubis-Kubiak A, Piwowar A (2022) Molecular Mechanism of Lipotoxicity as an Interesting Aspect in the Development of Pathological States-Current View of Knowledge. Cells 11 (5). doi:10.3390/cells11050844
5. Shimabukuro M, Higa M, Zhou YT, Wang MY, Newgard CB, Unger RH (1998) Lipoapoptosis in beta-cells of obese prediabetic fa/fa rats. Role of serine palmitoyltransferase overexpression. J Biol Chem 273 (49):32487–32490. doi:10.1074/jbc.273.49.32487

6. Parveen F, Bender D, Law SH, Mishra VK, Chen CC, Ke LY (2019) Role of Ceramidases in Sphingolipid Metabolism and Human Diseases. Cells 8 (12). doi:10.3390/cells8121573
7. Arana L, Gangoiti P, Ouro A, Trueba M, Gomez-Munoz A (2010) Ceramide and ceramide 1-phosphate in health and disease. Lipids Health Dis 9:15. doi:10.1186/1476-511X-9-15
8. Filippov V, Song MA, Zhang K, Vinters HV, Tung S, Kirsch WM, Yang J, Duerksen-Hughes PJ (2012) Increased ceramide in brains with Alzheimer's and other neurodegenerative diseases. J Alzheimers Dis 29 (3):537–547. doi:10.3233/JAD-2011-111202
9. Mielke MM, Bandaru VV, Haughey NJ, Xia J, Fried LP, Yasar S, Albert M, Varma V, Harris G, Schneider EB, Rabins PV, Bandeen-Roche K, Lyketsos CG, Carlson MC (2012) Serum ceramides increase the risk of Alzheimer disease: the Women's Health and Aging Study II. Neurology 79 (7):633–641. doi:10.1212/WNL.0b013e318264e380
10. Maedler K, Spinas GA, Dyntar D, Moritz W, Kaiser N, Donath MY (2001) Distinct effects of saturated and monounsaturated fatty acids on beta-cell turnover and function. Diabetes 50 (1):69–76. doi:10.2337/diabetes.50.1.69
11. Zhang S, Liu J, MacGibbon G, Dragunow M, Cooper GJ (2002) Increased expression and activation of c-Jun contributes to human amylin-induced apoptosis in pancreatic islet beta-cells. J Mol Biol 324 (2):271–285. doi:10.1016/s0022-2836(02)01044-6
12. Zhang G, Meng L, Wang Z, Peng Q, Chen G, Xiong J, Zhang Z (2022) Islet amyloid polypeptide cross-seeds tau and drives the neurofibrillary pathology in Alzheimer's disease. Mol Neurodegener 17 (1):12. doi:10.1186/s13024-022-00518-y
13. Zhang S, Liu J, Dragunow M, Cooper GJ (2003) Fibrillogenic amylin evokes islet beta-cell apoptosis through linked activation of a caspase cascade and JNK1. J Biol Chem 278 (52):52810–52819. doi:10.1074/jbc.M308244200
14. Konarkowska B, Aitken JF, Kistler J, Zhang S, Cooper GJ (2006) The aggregation potential of human amylin determines its cytotoxicity towards islet beta-cells. FEBS J 273 (15):3614–3624. doi:10.1111/j.1742-4658.2006.05367.x
15. Shimabukuro M, Zhou YT, Levi M, Unger RH (1998) Fatty acid-induced beta cell apoptosis: a link between obesity and diabetes. Proc Natl Acad Sci U S A 95 (5):2498–2502. doi:10.1073/pnas.95.5.2498
16. Tian H, Wang ZY (2019) Zinc Chelator Inhibits Zinc-Induced Islet Amyloid Polypeptide Deposition and Apoptosis in INS-1 Cells. Biol Trace Elem Res 189 (1):201–208. doi:10.1007/s12011-018-1444-5
17. Huang JS, Mukherjee JJ, Kiss Z (1999) Ethanol potentiates the mitogenic effects of sphingosine 1-phosphate by a zinc- and calcium-dependent mechanism in fibroblasts. Arch Biochem Biophys 366 (1):131–138. doi:10.1006/abbi.1999.1203
18. Song MK, Bischoff DS, Song AM, Uyemura K, Yamaguchi DT (2017) Metabolic relationship between diabetes and Alzheimer's Disease affected by Cyclo(His-Pro) plus zinc treatment. BBA Clin 7:41–54. doi:10.1016/j.bbacli.2016.09.003 S2214-6474(16)30039-3 [pii]

19. Prakash KR, Tang Y, Kozikowski AP, Flippen-Anderson JL, Knoblach SM, Faden AI (2002) Synthesis and biological activity of novel neuroprotective diketopiperazines. Bioorg Med Chem 10 (9):3043–3048. doi:10.1016/s0968-0896(02)00132-3
20. Prasad C (1995) Bioactive cyclic dipeptides. Peptides 16 (1):151–164. doi:10.1016/0196-9781(94)00017-z
21. Hilton CW, Prasad C, Vo P, Mouton C (1992) Food contains the bioactive peptide, cyclo(His-Pro). J Clin Endocrinol Metab 75 (2):375–378. doi:10.1210/jcem.75.2.1639938
22. Mizuma T, Koyanagi A, Awazu S (1997) Intestinal transport and metabolism of analgesic dipeptide, kyotorphin: rate-limiting factor in intestinal absorption of peptide as drug. Biochim Biophys Acta 1335 (1–2):111–119. doi:10.1016/s0304-4165(96)00128-6
23. Banks WA, Kastin AJ, Jaspan JB (1992) Orally administered cyclo(His-Pro) reduces ethanol-induced narcosis in mice. Pharmacol Biochem Behav 43 (3):939–941. doi:10.1016/0091-3057(92)90428-i
24. Banks WA, Kastin AJ, Akerstrom V, Jaspan JB (1993) Radioactively iodinated cyclo(His-Pro) crosses the blood-brain barrier and reverses ethanol-induced narcosis. Am J Physiol 264 (5 Pt 1):E723-729. doi:10.1152/ajpendo.1993.264.5.E723
25. Jaspan JB, Banks WA, Kastin AJ (1994) Study of passage of peptides across the blood-brain barrier: biological effects of cyclo(His-Pro) after intravenous and oral administration. Ann N Y Acad Sci 739:101–107. doi:10.1111/j.1749-6632.1994.tb19811.x
26. Acun AD, Kantar D, Er H, Erkan O, Derin N, Yargicoglu P (2023) Investigation of Cyclo-Z Therapeutic Effect on Insulin Pathway in Alzheimer's Rat Model: Biochemical and Electrophysiological Parameters. Mol Neurobiol. doi:10.1007/s12035-023-03334-7
27. Wang X, Hu X, Yang Y, Takata T, Sakurai T (2015) Systemic pyruvate administration markedly reduces neuronal death and cognitive impairment in a rat model of Alzheimer's disease. Exp Neurol 271:145–154. doi:10.1016/j.expneurol.2015.06.008
28. Song MK, Rosenthal MJ, Song AM, Uyemura K, Yang H, Ament ME, Yamaguchi DT, Cornford EM (2009) Body weight reduction in rats by oral treatment with zinc plus cyclo-(His-Pro). Br J Pharmacol 158 (2):442–450. doi:10.1111/j.1476-5381.2009.00201.x
29. Li Y, Duffy KB, Ottinger MA, Ray B, Bailey JA, Holloway HW, Tweedie D, Perry T, Mattson MP, Kapogiannis D, Sambamurti K, Lahiri DK, Greig NH (2010) GLP-1 receptor stimulation reduces amyloid-beta peptide accumulation and cytotoxicity in cellular and animal models of Alzheimer's disease. J Alzheimers Dis 19 (4):1205–1219. doi:10.3233/JAD-2010-1314
30. Gong L, Li SL, Li H, Zhang L (2011) Ginsenoside Rg1 protects primary cultured rat hippocampal neurons from cell apoptosis induced by beta-amyloid protein. Pharm Biol 49 (5):501–507. doi:10.3109/13880209.2010.521514
31. Wijesekara N, Goncalves RA, De Felice FG, Fraser PE (2018) Impaired peripheral glucose homeostasis and Alzheimer's disease. Neuropharmacology 136 (Pt B):172–181. doi:10.1016/j.neuropharm.2017.11.027

32. Ekblad LL, Johansson J, Helin S, Viitanen M, Laine H, Puukka P, Jula A, Rinne JO (2018) Midlife insulin resistance, APOE genotype, and late-life brain amyloid accumulation. Neurology 90 (13):e1150-e1157. doi:10.1212/WNL.0000000000005214
33. Craft S, Newcomer J, Kanne S, Dagogo-Jack S, Cryer P, Sheline Y, Luby J, Dagogo-Jack A, Alderson A (1996) Memory improvement following induced hyperinsulinemia in Alzheimer's disease. Neurobiol Aging 17 (1):123–130. doi:10.1016/0197-4580(95)02002-0
34. Acun AD, Kantar D, Er H, Erkan O, Derin N, Yargicoglu P (2023) Investigation of Cyclo-Z Therapeutic Effect on Insulin Pathway in Alzheimer's Rat Model: Biochemical and Electrophysiological Parameters. Mol Neurobiol 60 (7):4030–4048. doi:10.1007/s12035-023-03334-7
35. Willette AA, Johnson SC, Birdsill AC, Sager MA, Christian B, Baker LD, Craft S, Oh J, Statz E, Hermann BP, Jonaitis EM, Koscik RL, La Rue A, Asthana S, Bendlin BB (2015) Insulin resistance predicts brain amyloid deposition in late middle-aged adults. Alzheimers Dement 11 (5):504–510 e501. doi:10.1016/j.jalz.2014.03.011
36. Clarke JR, Lyra ESNM, Figueiredo CP, Frozza RL, Ledo JH, Beckman D, Katashima CK, Razolli D, Carvalho BM, Frazao R, Silveira MA, Ribeiro FC, Bomfim TR, Neves FS, Klein WL, Medeiros R, LaFerla FM, Carvalheira JB, Saad MJ, Munoz DP, Velloso LA, Ferreira ST, De Felice FG (2015) Alzheimer-associated Abeta oligomers impact the central nervous system to induce peripheral metabolic deregulation. EMBO Mol Med 7 (2):190–210. doi:10.15252/emmm.201404183
37. Sartorius T, Peter A, Heni M, Maetzler W, Fritsche A, Haring HU, Hennige AM (2015) The brain response to peripheral insulin declines with age: a contribution of the blood-brain barrier? PLoS One 10 (5):e0126804. doi:10.1371/journal.pone.0126804
38. Czubowicz K, Jesko H, Wencel P, Lukiw WJ, Strosznajder RP (2019) The Role of Ceramide and Sphingosine-1-Phosphate in Alzheimer's Disease and Other Neurodegenerative Disorders. Mol Neurobiol 56 (8):5436–5455. doi:10.1007/s12035-018-1448-3
39. Zhang Y, Zhou B, Deng B, Zhang F, Wu J, Wang Y, Le Y, Zhai Q (2013) Amyloid-beta induces hepatic insulin resistance in vivo via JAK2. Diabetes 62 (4):1159–1166. doi:10.2337/db12-0670
40. Miklossy J, Qing H, Radenovic A, Kis A, Vileno B, Laszlo F, Miller L, Martins RN, Waeber G, Mooser V, Bosman F, Khalili K, Darbinian N, McGeer PL (2010) Beta amyloid and hyperphosphorylated tau deposits in the pancreas in type 2 diabetes. Neurobiol Aging 31 (9):1503–1515. doi:10.1016/j.neurobiolaging.2008.08.019
41. Roher AE, Esh CL, Kokjohn TA, Castano EM, Van Vickle GD, Kalback WM, Patton RL, Luehrs DC, Daugs ID, Kuo YM, Emmerling MR, Soares H, Quinn JF, Kaye J, Connor DJ, Silverberg NB, Adler CH, Seward JD, Beach TG, Sabbagh MN (2009) Amyloid beta peptides in human plasma and tissues and their significance for Alzheimer's disease. Alzheimers Dement 5 (1):18–29. doi:10.1016/j.jalz.2008.10.004
42. Wijesekara N, Ahrens R, Sabale M, Wu L, Ha K, Verdile G, Fraser PE (2017) Amyloid-beta and islet amyloid pathologies link Alzheimer's disease and type 2 diabetes in a transgenic model. FASEB J 31 (12):5409–5418. doi:10.1096/fj.201700431R

43. Oskarsson ME, Paulsson JF, Schultz SW, Ingelsson M, Westermark P, Westermark GT (2015) In vivo seeding and cross-seeding of localized amyloidosis: a molecular link between type 2 diabetes and Alzheimer disease. Am J Pathol 185 (3):834–846. doi:10.1016/j.ajpath.2014.11.016
44. Moreno-Gonzalez I, Edwards Iii G, Salvadores N, Shahnawaz M, Diaz-Espinoza R, Soto C (2017) Molecular interaction between type 2 diabetes and Alzheimer's disease through cross-seeding of protein misfolding. Mol Psychiatry 22 (9):1327–1334. doi:10.1038/mp.2016.230
45. Schultz N, Janelidze S, Byman E, Minthon L, Nagga K, Hansson O, Wennstrom M (2019) Levels of islet amyloid polypeptide in cerebrospinal fluid and plasma from patients with Alzheimer's disease. PLoS One 14 (6):e0218561. doi:10.1371/journal.pone.0218561
46. Kimura N (2016) Diabetes Mellitus Induces Alzheimer's Disease Pathology: Histopathological Evidence from Animal Models. Int J Mol Sci 17 (4):503. doi:10.3390/ijms17040503
47. Bharadwaj P, Wijesekara N, Liyanapathirana M, Newsholme P, Ittner L, Fraser P, Verdile G (2017) The Link between Type 2 Diabetes and Neurodegeneration: Roles for Amyloid-beta, Amylin, and Tau Proteins. J Alzheimers Dis 59 (2):421–432. doi:10.3233/JAD-161192
48. Ly H, Verma N, Sharma S, Kotiya D, Despa S, Abner EL, Nelson PT, Jicha GA, Wilcock DM, Goldstein LB, Guerreiro R, Bras J, Hanson AJ, Craft S, Murray AJ, Biessels GJ, Troakes C, Zetterberg H, Hardy J, Lashley T, Aesg, Despa F (2021) The association of circulating amylin with beta-amyloid in familial Alzheimer's disease. Alzheimers Dement (N Y) 7 (1):e12130. doi:10.1002/trc2.12130
49. Custodia A, Romaus-Sanjurjo D, Aramburu-Nunez M, Alvarez-Rafael D, Vazquez-Vazquez L, Camino-Castineiras J, Leira Y, Pias-Peleteiro JM, Aldrey JM, Sobrino T, Ouro A (2022) Ceramide/Sphingosine 1-Phosphate Axis as a Key Target for Diagnosis and Treatment in Alzheimer's Disease and Other Neurodegenerative Diseases. Int J Mol Sci 23 (15). doi:10.3390/ijms23158082
50. Jazvinscak Jembrek M, Hof PR, Simic G (2015) Ceramides in Alzheimer's Disease: Key Mediators of Neuronal Apoptosis Induced by Oxidative Stress and Abeta Accumulation. Oxid Med Cell Longev 2015:346783. doi:10.1155/2015/346783
51. Ito M, Okino N, Tani M (2014) New insight into the structure, reaction mechanism, and biological functions of neutral ceramidase. Biochim Biophys Acta 1841 (5):682–691. doi:10.1016/j.bbalip.2013.09.008
52. Lei X, Zhang S, Bohrer A, Bao S, Song H, Ramanadham S (2007) The group VIA calcium-independent phospholipase A2 participates in ER stress-induced INS-1 insulinoma cell apoptosis by promoting ceramide generation via hydrolysis of sphingomyelins by neutral sphingomyelinase. Biochemistry 46 (35):10170–10185. doi:10.1021/bi700017z
53. Zhang X, Wu J, Dou Y, Xia B, Rong W, Rimbach G, Lou Y (2012) Asiatic acid protects primary neurons against C2-ceramide-induced apoptosis. Eur J Pharmacol 679 (1–3):51–59. doi:10.1016/j.ejphar.2012.01.006
54. Kizhakkayil J, Thayyullathil F, Chathoth S, Hago A, Patel M, Galadari S (2012) Glutathione regulates caspase-dependent ceramide production and curcumin-induced apoptosis in human leukemic cells. Free Radic Biol Med 52 (9):1854–1864. doi:10.1016/j.freeradbiomed.2012.02.026

55. Park SW, Choi SA, Yun JW, Choi JW (2012) Alterations in pancreatic protein expression in STZ-induced diabetic rats and genetically diabetic mice in response to treatment with hypoglycemic dipeptide Cyclo (His-Pro). Cell Physiol Biochem 29 (3–4):603–616. doi:10.1159/000338514
56. Celer M, Mogulkoc R, Baltaci AK, Dasdelen D (2018) The effects of zinc and melatonin on muscle ischaemi-reperfusion injury in rat. Cell Mol Biol (Noisy-le-grand) 64 (3):1–4. doi:10.14715/cmb/2018.64.3.1
57. Ueda N (2022) A Rheostat of Ceramide and Sphingosine-1-Phosphate as a Determinant of Oxidative Stress-Mediated Kidney Injury. Int J Mol Sci 23 (7). doi:10.3390/ijms23074010
58. Sano H, Eguez L, Teruel MN, Fukuda M, Chuang TD, Chavez JA, Lienhard GE, McGraw TE (2007) Rab10, a target of the AS160 Rab GAP, is required for insulin-stimulated translocation of GLUT4 to the adipocyte plasma membrane. Cell Metab 5 (4):293–303. doi:10.1016/j.cmet.2007.03.001

Figures

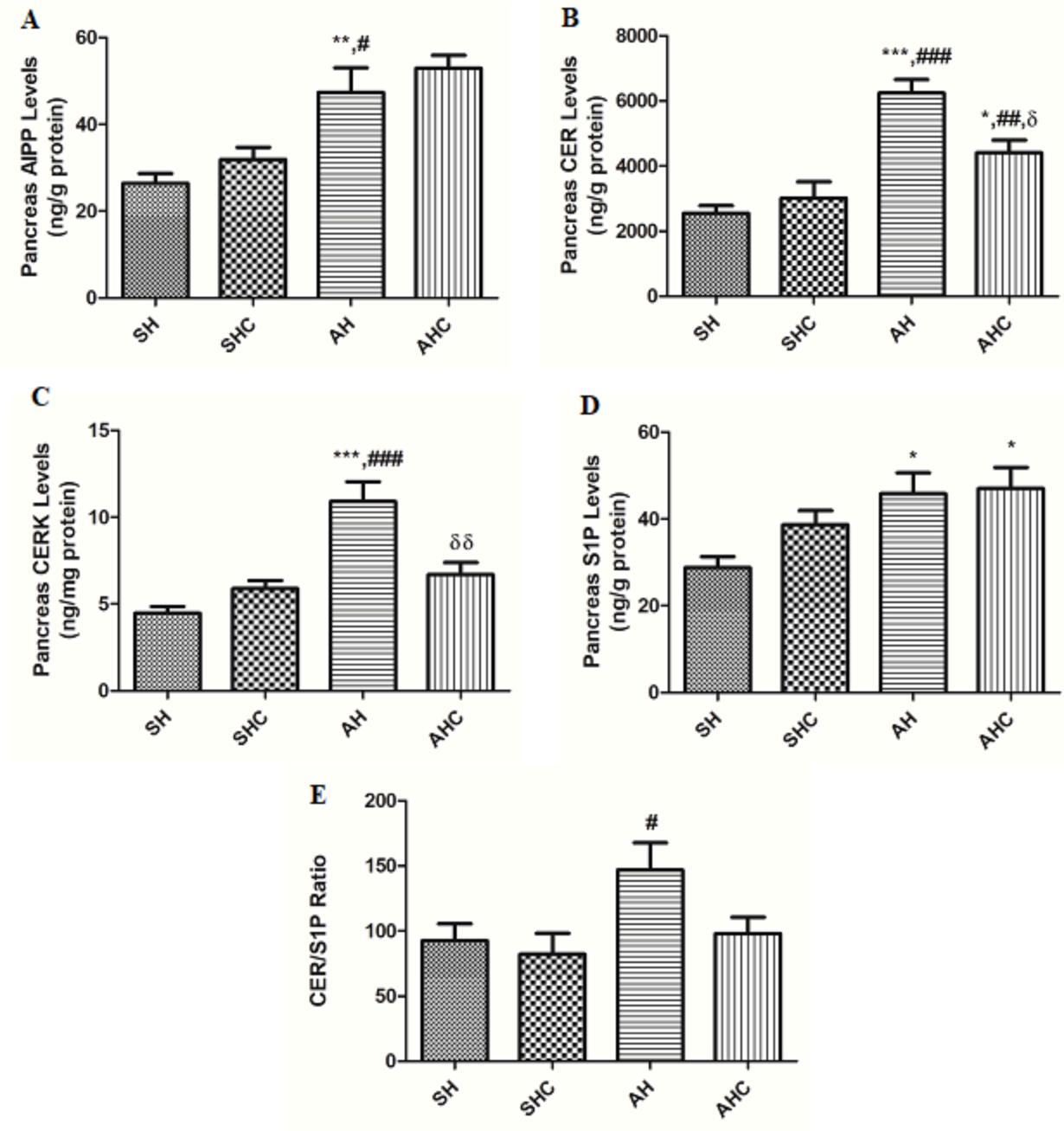

Figure 1

A: Pancreas AIPP levels in SH and experimental groups, n=6; B: Pancreas CER levels in SH and experimental groups, n=6; C: Pancreas S1P levels in SH and experimental groups, n=6; D: Pancreas CERK levels in SH and experimental groups, n=6; E: Pancreas CER/S1P ratio in SH and experimental groups, n=6. Results are presented as mean ±SEM. (*: Significant vs SH group, #: Significant vs SHZ group, δ: Significant vs AD group. *: $p<0.05$; **: $p<0.01$; ***: $p<0.001$, #: $p<0.05$; ##: $p<0.01$; ###: $p<0.001$, δ: $p<0.05$, δδ: $p<0.01$, δδδ: $p<0.001$)

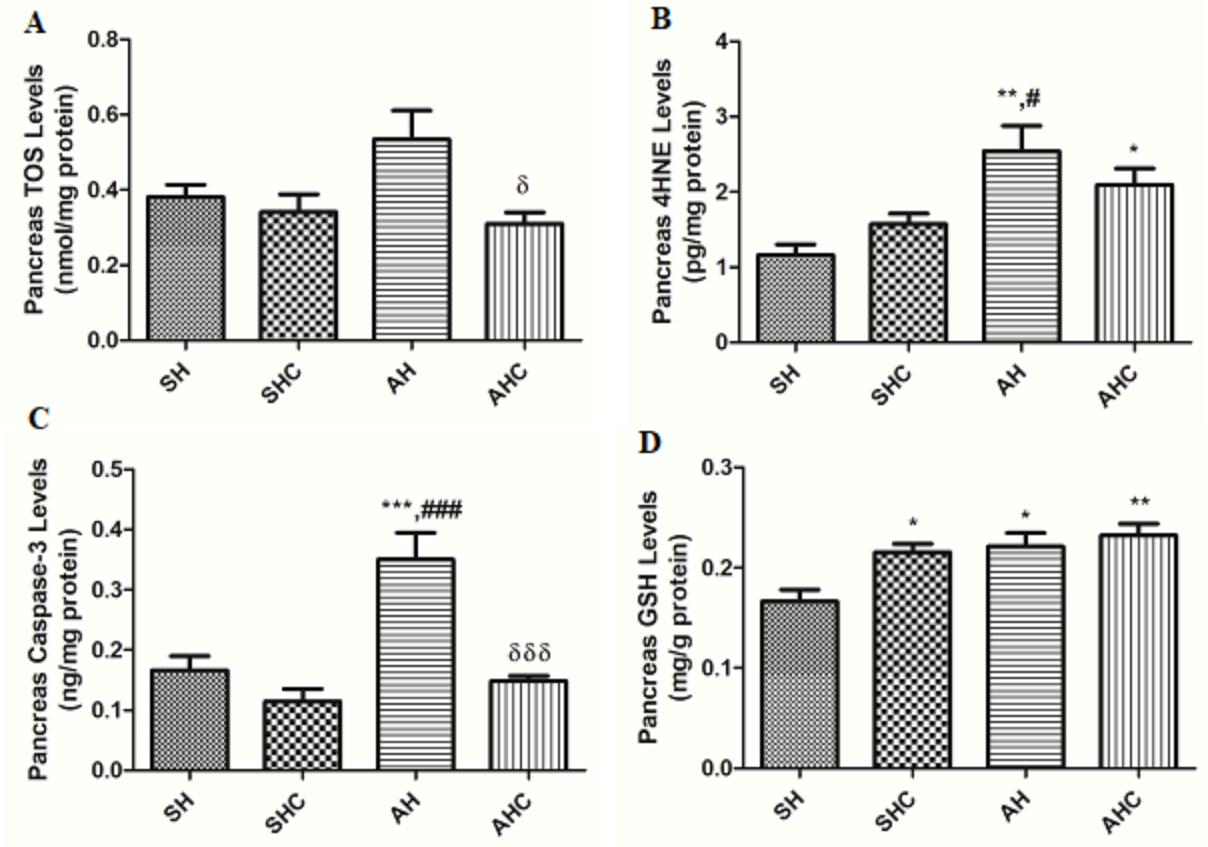

Figure 2

A: Pancreas TOS levels in SH and experimental groups, n=6; B: Pancreas 4HNE levels in SH and experimental groups, n=6; C: Pancreas caspase-3 levels in SH and experimental groups, n=6; D: Pancreas GSH levels in SH and experimental groups, n=6. Results are presented as mean ±SEM. (*: Significant vs SH group, #: Significant vs SHZ group, δ: Significant vs AD group. *: $p<0.05$; **: $p<0.01$; ***: $p<0.001$, #: $p<0.05$; ##: $p<0.01$; ###: $p<0.001$, δ: $p<0.05$, δδ: $p<0.01$, δδδ: $p<0.001$)

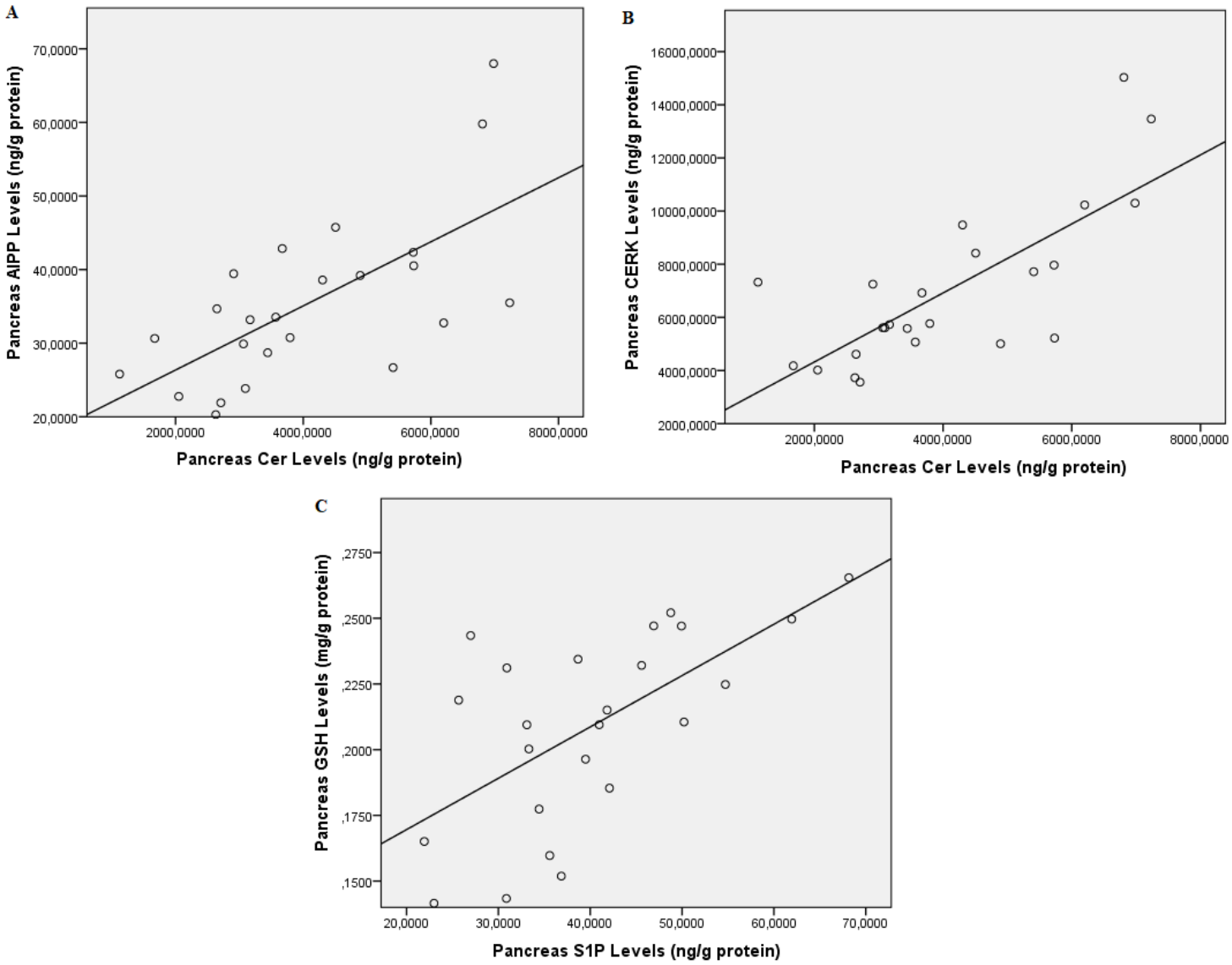

Figure 3

A: The correlations between pancreas CER levels and pancreas AIPP levels (Pearson r= 0.663, p<0.001, N=24); B: The correlations between pancreas CER levels and pancreas CERK levels (Pearson r= 0.754, p<0.001, N=24); C: The correlations between pancreas S1P levels and pancreas GSH levels(Pearson r= 0.624, p<0.001, N=24).